3D reconstruction of underwater scenes using image sequences from acoustic camera

Naouraz Brahim*†, Didier Guériot*, Sylvie Daniel† and Basel Solaiman*
*Institut TELECOM ; TELECOM Bretagne
Technopôle Brest-Iroise, CS 83818, 29238 Brest Cedex 3, France
†Département des sciences géomatiques
Université Laval, Québec, Canada

***Abstract*—This paper introduces a system for three-dimensional (3D) reconstruction of underwater environments using multiple images acquired by an acoustical camera from different points of view. The final target of the work is to produce a full 3D representation of the observed environment to improve its exploration and analysis. Indeed, as the DIDSON acoustic camera provides sequences of 2D images (distance and azimuth), the challenge consists in determining the missing elevation information about the observed scene in order to reconstruct (x,y,z) models, together with the geometrical transformation parameters between the acquisition view points, using image information only. Our research work is in its early stage, the work presented in this paper is particularly focused on the first step of the 3D reconstruction system which is feature point extraction as feature points must represent the scene geometrical characteristics. Thus, the proposed methodology is based on corner detection from extracted contours. However, speckle noise introduces local, non-geometrically relevant contours that should be removed. Embedded within a multi-scale edge analysis approach, analyzing extracted contours from several consecutive images allows relevant contours selection. This methodology applied to real and simulated images, shows promising results to complete the full 3D reconstruction process.**

***Index Terms*—3D reconstruction, acoustic camera, contour extraction, feature matching**

I. Introduction

The main purpose of the proposed work is to develop a method that enables 3D reconstruction of underwater scenes using sequences of acoustic images. Environment 3D reconstruction will be useful for visual search, inspection and survey which are critical in a number of underwater applications in marine sciences, observation, maintenance, or repairing of undersea structures. Indeed, according to recent studies, climate changes significantly impact our marine environment with temperature increases, chemistry modifications, ocean circulation perturbation influencing population dynamics and underwater structure stability. Thus, monitoring these changes within the marine environment becomes one of the current challenges for underwater exploration.

The most common technique used by geologists, biologists or surveillance teams to observe and analyze underwater scene features, relies on vision-based systems either acoustical or optical, mounted on autonomous underwater vehicles (AUVs). Optical cameras are widely used for acquiring images of the sea-floor/underwater structures as the images they collect provide information about the physical properties of the observed scene (color, reflection, geometry). However, their ranges are rather limited without external sources of light and almost non-existent with high turbidity. These non-ideal underwater conditions (dark and turbid waters) are frequently encountered in harbors or deep waters, making acoustic imaging the most reliable means to get information from underwater environments.

Consequently, acoustic active sonar systems are presently the most extensively used systems for underwater image generation. The main advantage compared to video cameras is that they can operate at much longer ranges (up to several hundred meters) with lower resolutions. On this study, we will focus on high frequency acoustic cameras that have a shorter range (a few meters) but produce high resolution images (a few centimeters or so, per pixel). In addition, they are almost not affected by turbid waters, ensuring that details and information about the scene are properly acquired. However, these acoustic cameras only collect backscattered energy according to range and azimuth. Thus, using only one acquired image does not allow to compute scene elevation corresponding to each image pixel, even with high resolution. Each collected image giving an elevation ambiguous 2D representation of the observed environment, it would be very attractive to design a system which can gather all these partial views in order to compute the missing dimension and provide height information about the scene. This is the purpose of our work which consists in developing a methodology to retrieve 3D information from acoustic images and offer 3D environment reconstruction permitting observation and monitoring of underwater scene.

This paper will focus on the first stage of the full methodology which is robust features extraction. The actual acoustic camera is presented in Section II. Section III presents the complete methodology and indicates how computing corresponding contours (Section IV) and robust features detection (Section V) fit in this scheme.

II. Acquiring images with DIDSON acoustic camera

The acoustic camera discussed in this paper is the Dual-frequency Identification Sonar (DIDSON) [1]. Depending on the sonar frequency, either 1.0 MHz (for LR mode) or 1.8 MHz (for HR mode), DIDSON ranges from half a meter to 25 meters and forms 48 or 96 beams in the horizontal plane, each

978-1-4244-5222-4/10/$26.00 ©2010 IEEE

beam being 0.3° width with spacing ranging from 0.3° to 0.4°, for a full 29° azimuth coverage. As a front-looking sonar, the elevation aperture is 10.8° with fixed vertical tilt angle. Thus, the system produces either 48×512 or 96×512 azimuth-by-range images where each pixel contains the backscattered energy for all the points in the scene located at the same distance with the same azimuth from the camera. No information about the elevation is recorded [2]. Figure 1 illustrates how the polar collected image can be interpreted in relation to the spatial camera configuration.

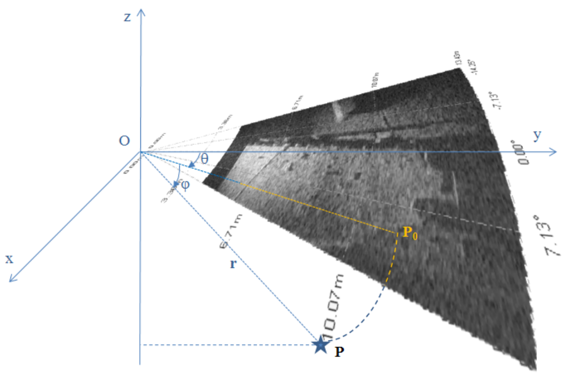

Fig. 1. Referencing acquired image within the camera (x,y,z) reference

Depending on the operating frequency and the maximum selected range, DIDSON images refresh rate ranges from 4 frames/s to 21 frames/s. Then, multiple images from the same underwater scene can be produced with different viewpoints as the camera moves in the scene. It gives materials to perform 3D scene reconstruction from images. However, as for all acoustic sensors, various phenomena like speckle noise, strongly affect the collected image quality, requiring further image processing like edge detection, to be more robust.

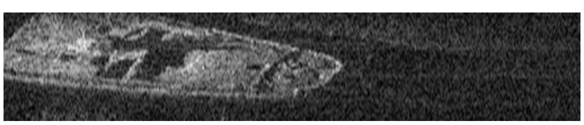

(a) Ship (frame 64)

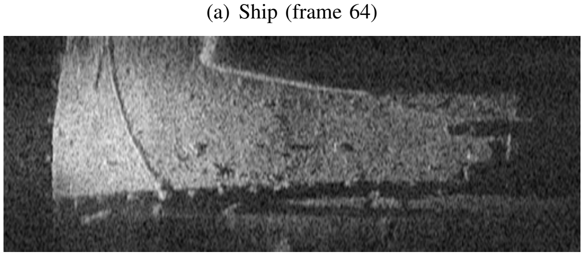

(b) Bridge (frame 95)

Fig. 2. Raw DIDSON frames extracted from image sequences

Figure 2 presents two frames extracted from two sequences used in this paper. LR mode was used for the first one, *Ship*, producing 48 lines images while the *Bridge* sequence has been recorded in HR mode with twice the amount of lines for the same angular coverage. Azimuth resolution is then twice finer for the *Bridge* sequence.

III. 3D Reconstruction Methodology

In this study, the DIDSON acoustic camera has been used because of the previously described features (high resolution, rapid refresh rates allowing real-time underwater image sequences). In these sequences, the same scene appears in different successive images from different points of view. Thus, the proposed research work addressed in this paper aims at developing a method that exploits image information redundancy to reconstruct the observed scene.

A. From successive sonar images to 3D reconstructed environment

As shown in Figure 3, this paper introduces a 3D reconstruction method inspired from stereovision techniques, even if the acoustic camera acquisition geometry (azimuth and range are recorded, no elevation) does not fit optical camera acquisition geometry where azimuth and elevation are known, not range.

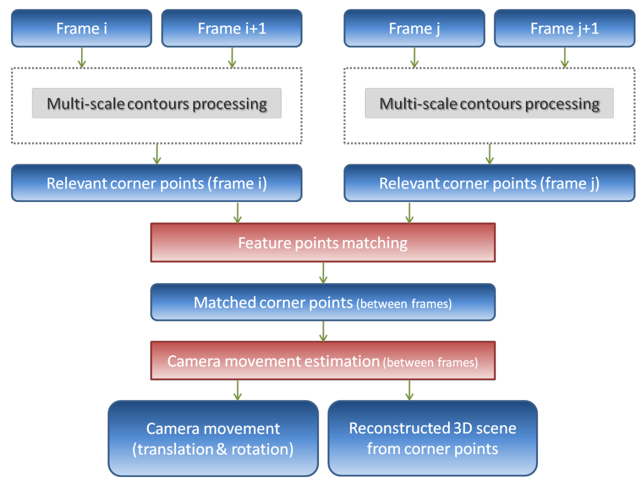

Fig. 3. 3D scene reconstruction global methodology inspired from stereovision processing

The global processing consists in three steps:

1) *Features detection & selection*: It is mandatory that this step provides sets of points that represent some salient features of the scene to be reconstructed. Moreover, the extracted points from one image should be consistent with extracted points from another image observing the same scene geographic features, in order to allow the best possible matching. How to obtain such sets of robust features will be detailed in section III-B.
2) *Selected features matching*: Extracted points from two images observing the same scene should correspond to same salient features from this scene. A matching step creates such links between datasets taking care of problems like occlusion or too drastic point of view changes. In that case, a bijection between the two sets is not guaranteed.
3) *3D reconstruction from matched features*: Once the sets of points matched, minimizing the distance between the reconstructed points from image 1 and from image 2 according to the supposed inter-acquisition geometry,

allows to find the best geometrical transformation between the two acquisition points of view (both rotation & translation). Knowing this transformation, computing (x,y,z) coordinates of scene locations from other pairs of points, is rather straightforward.

This paper will not present the full methodology but focus on the crucial scene relevant features detection process, assuming the same scene is observed.

B. Focusing on extracting robust scene relevant features from images

As already presented, robust features points need to be extracted from collected images in order to participate in the computation of the geometrical transformation between the acquisition view points. Indeed, they need to represent salient features of the scene like ending edges, in order for these features to be unambiguously identified on the images. Thus, the detection procedure should be accurate (at the sensor resolution) and each paired of remaining points clearly associated to one unique geographic location in the scene.

As illustrated in Figure 4, to achieve such detection goals, a procedure based on a multi-scale edges characterization, is proposed:

1) *Edge extraction*: Robust feature points clearly belong to object edges in the collected images. The first step consists in extracting such edges from images so that all the features are detected. Section IV-A discusses the procedure.
2) *Reducing noise impact*: Speckle noise and artifacts in acoustic images introduce local, non-geometrically relevant contours. Therefore, it is required to remove these false contours while preserving scene object contours. The proposed strategy consists in comparing extracted edges from two closely acquired images assuming the point of view hasn't changed much. Contours that don't match between images result from noise impact when considering independent noise contribution from one image to another. If they match, even partially, they are probably involved by the scene. Indeed, due to the rapid refresh rates of DIDSON camera, the displacement estimated between two successive images usually stays under 2 pixels difference. Thus this step allows to discard contours coming from noise and create a list of corresponding contours between the contours extracted from the two images. Section IV-B gives more details about noise reduction impact.
3) *Focusing on strong features*: Non-redundant contours have been deleted. However, our main interest is to extract salient points from the scene. It is mandatory to be sure that the extracted points correspond unambiguously to same scene points. To get this information, a multi-scale analysis has been introduced in order to detect the strong main scene features on the images i.e. those having an impact even after filtering out image details. However, the last scale to consider needs to be automatically found. The remaining corresponding contours are those from the highest resolution level still appearing at the most filtered level. It insures the contours actually reflect strong scene features as explained in Section IV-C.
4) *Corner points extraction*: Once the corresponding contours has been extracted, extracting relevant corner points consists in searching for the highest curvature points on these contours. These points will indicate salient scene features as they correspond to contour direction changes.

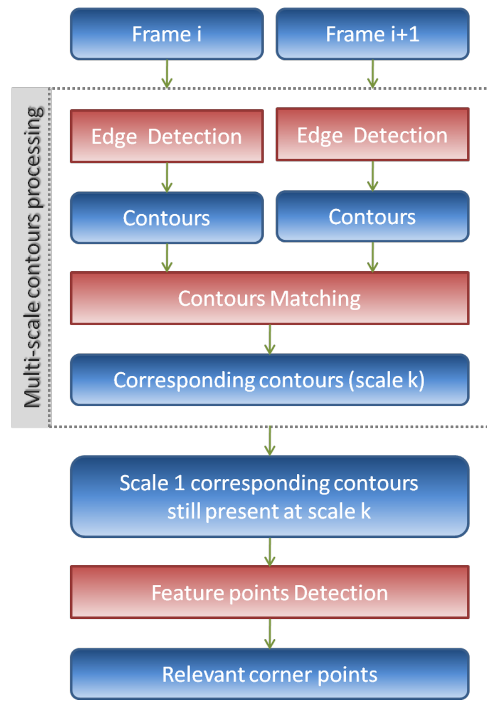

Fig. 4. Extracting scene relevant features for 3D reconstruction

IV. Computing Corresponding Contours

Covering the first step of the proposed methodology, this section presents the multi-scale algorithm dedicated to extract corresponding contours from close frames, taking into account noise impact on these frames. First, contours are extracted from every image. The same contours appearing on successive images are matched and preserved as representation of scene geometric features. Contours coming from noise are deleted in the process. These corresponding contours are computed for various image scales obtained through Gaussian filtering, in order to only preserve strongly relevant contours linked to the scene geometry.

A. Edge detection

According to the definition proposed by Canny [3], edges are defined as particular points where the gradient vector modulus is locally maximal in the gradient vector direction. The Canny filter which is considered as an optimal edge detector, permits to extract such points. Applied on a gray scale image, it yields an image showing the positions of tracked intensity discontinuities. Indeed, it works as a multi-stage process: first, the image is smoothed by a Gaussian convolution. A simple 2D first derivative operator is then applied to the smoothed image in order to highlight regions with high first spatial derivatives. Doing that, edges give rise to ridges in the gradient magnitude image. The algorithm then tracks along the top of these ridges and sets to zero all pixels that are not actually on the ridge top so as to output a thin line (non-maximal suppression). The tracking process exhibits hysteresis controlled by two thresholds: T_1 and T_2, with $T_1 > T_2$. Tracking can only begin at a point on a ridge higher than T_1. Then it continues in both directions out from that point until the height of the ridge falls below T_2. This hysteresis helps to ensure that noisy edges are not broken up into multiple edge fragments.

(a) Frame i

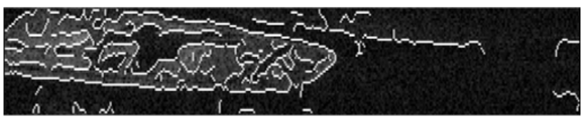

(b) Frame i+1

Fig. 5. Contours extraction through Canny edge detector on two successive frames from *Ship* sequence

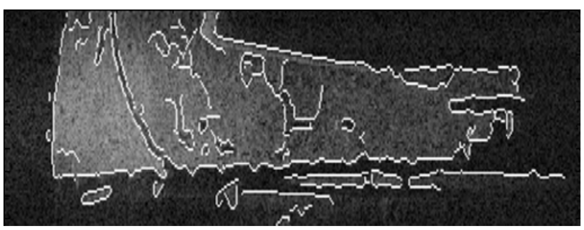

(a) Frame i

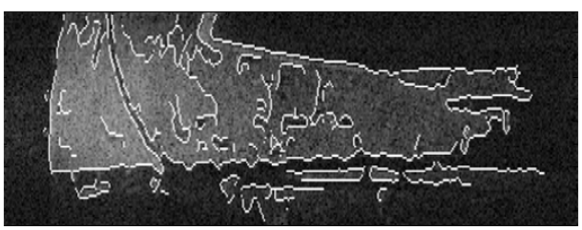

(b) Frame i+1

Fig. 6. Contours extraction through Canny edge detector on two successive frames from *Bridge* sequence

Figures 5 and 6 shows results of the Canny edge detector applied to two successive images from each reference sequences. According to the described algorithm, this edge detector produces contours on which the final corner points are located. However, even if it is quite resistant to noise compared to other edge detector filters (Prewitt, Sobel, ...), several extra contours coming from noise are observed.

B. Edge matching for finding corresponding contours

Thus, to remove false contours (coming from noise), a contour matching approach has been developed based on the percentage of contour points existing in the corresponding image within a small neighborhood, for each contour. This matching algorithm requires a small camera displacement between the two successive images to be able to find in image 2, within a small neighborhood, a corresponding contour for contours from image 1. This hypothesis is clearly checked within our framework.

To estimate if a contour $\mathcal{C}_k^1$ from the list $\mathcal{C}^1$ of contours extracted from image 1 has a corresponding contour in image 2, the normalized matching contour length measure $\mathcal{M}$ is introduced in Equation 1. The normalized matching contour length $\mathcal{M}_k^{1\to 2}$ gives the amount of pixels from contour $\mathcal{C}_k^1$ having a corresponding contour pixel in image 2, within a small neighborhood. This measure is pixel-oriented as the previous edge extraction does not guarantee to have same length contours on each image.

$$\mathcal{M}_k^{1\to 2} = \frac{\sum_{p\in\mathcal{C}_k^1} \mathbb{1}_{\eta(p)\in\mathcal{C}^2}}{\ell(\mathcal{C}_k^1)} \tag{1}$$

where

- $\ell(\mathcal{C}_k^j)$ gives the length of contour $\mathcal{C}_k^j$,
- p stands for a (i, j) location in image 1 and 2,
- $\eta(p)$ defines a small neighborhood around p location in image 2,
- $\mathbb{1}_x = 1$ if x is true, 0 if not.

In this paper, as only close frames are considered without any other knowledge, standard 3×3 neighborhood is used. However, depending on a priori knowledge (camera displacement between the two acquisitions), η function can be tuned to be more oriented according to an estimated shift between the two images.

Histograms from Figures 7 and 8 give the computed $\mathcal{M}^{1\to 2}$ measure, for each extracted contour from Ship and Bridge sequences. Results show that $\mathcal{M}$ values for corresponding contours are higher than 50% while contours coming from noise remain under 25%. Indeed, scene features involve redundant contours within close frames, acquisition noise does not. Thus, only corresponding contours are preserved for extracting corner points. Images from Figures 7 and 8 present the corresponding contours for both frame i and $i + 1$ using $\mathcal{M}^{i\to i+1}$ for the first image and $\mathcal{M}^{i+1\to i}$ for the second. As previously mentioned, $\mathcal{M}$ measure is pixel-oriented involving that measure is not symmetrical.

Moreover, fixing the value for this threshold does not require a sharp technique. In this paper, a 25% threshold is used but histograms illustrate that slightly changing this value does not change the results drastically.

C. Focusing on relevant contours through multi-scale analysis

The previous step deals with removing contours coming from noise or artifacts using inter-images analysis. However, the final goal is to extract corners from contours with a strong

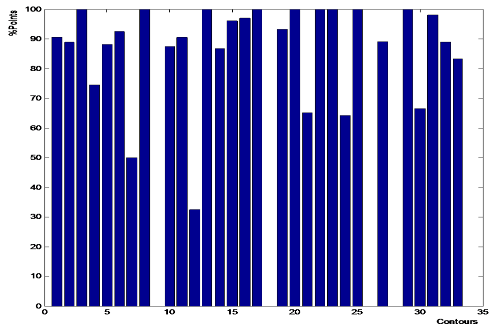

(a) Normalized matching contour length

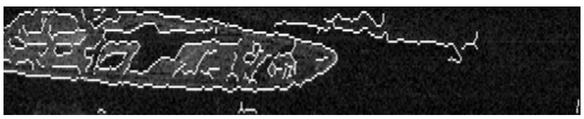

(b) Frame i

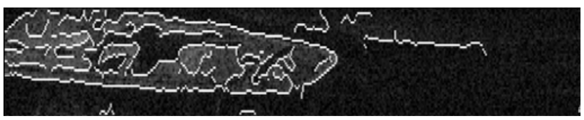

(c) Frame i+1

Fig. 7. Corresponding contours between consecutive frames from *Ship* sequence

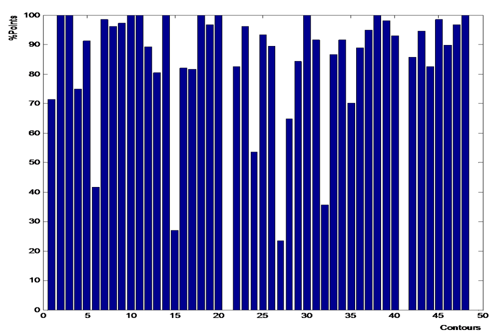

(a) Normalized matching contour length

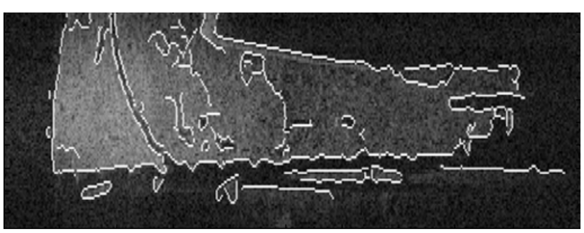

(b) Frame i

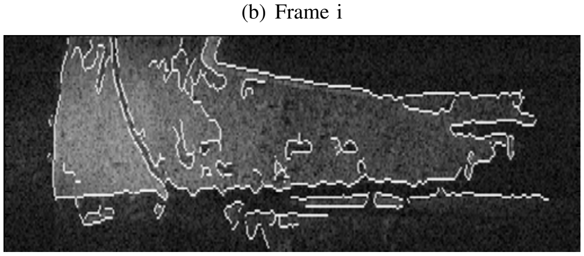

(c) Frame i+1

Fig. 8. Corresponding contours between consecutive frames from *Bridge* sequence

belief that these corners correspond to precise and unique scene features or salient points. Thus, this step will focus on eliminating weak contours, to preserve only robust contours that will produce robust corners and accurate camera pose estimation. To do so, we choose to analyze corresponding contours through a multi-scale approach.

1) Proposed algorithm: The proposed approach consists in computing corresponding contours for several different image scales. Images at different scales are obtained through Gaussian filtering with successive standard deviation increases. Corresponding contours are extracted on each scale. In order to automatically determine the last analysis scale n, corresponding contours are tracked from scale 1 (original image) to subsequent scales till the number of detected corresponding contours becomes stable over several scales.

Only scale 1 contours still appearing as corresponding contours in scale n are robust enough and preserved to participate in the corners detection.

2) Results: This multi-scale analysis has been performed on both Ship and Bridge sequences as shown in Figures 9 and 10. Through this multi-scale analysis, shapes of extracted corresponding contours become smoother; however, their occurrence characterizes sharp transitions between homogeneous regions in the images. These features are clearly interesting candidates for our application because of their robustness (after several scale filtering, only relevant features remain).

Logically, as presented with Figures 9 and 10 curves which give the evolution of the number of corresponding contours through successive scales, the number of corresponding contours decreases from scale to scale, till remaining stable when all the small and weak features have been removed. The last scale for the Ship sequence appears to be 6 while scale 8 seems to be the first stable scale of the series on the Bridge sequence.

Last scales automatically determined from multi-scale contour analysis on these two sequences are different. Indeed, the operating frequency modes used to acquire those sequences are different: LR for Ship sequence, HR for Bridge sequence. In HR mode, the beams number is twice the amount of HR mode beams, for the same azimuth coverage, bringing finer details. It then possible to get deeper scales before having a stable behavior.

For each sequence, once the last scale n has been determined, only the original corresponding contours (at scale 1) tracked from scale to scale and still appearing at scale n are preserved as shown in the last images in Figures 9 and 10. These corresponding contours will be considered as input for the next step (corners detection). Thus the proposed multi-scale analysis preserves only contours that characterize strong and relevant intensity changes, through tracking contours from scale to scale. However, as corner detection will be fed by scale 1 contours, it also preserves contours accurate localization.

As highlighted in Figure 9 (dotted yellow circle), some corresponding contours may be detected with a rather high normalized matching contour length measure. However, this measure being global to the contour, it does not reflect inho-

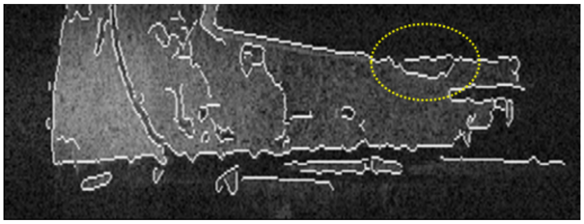

(a) Scale 1 (original corresponding contours)

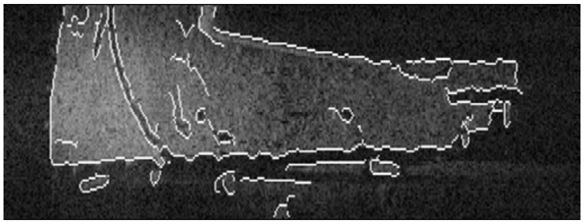

(b) Scale 2

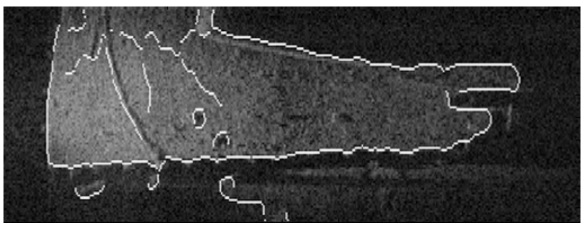

(c) Scale 6

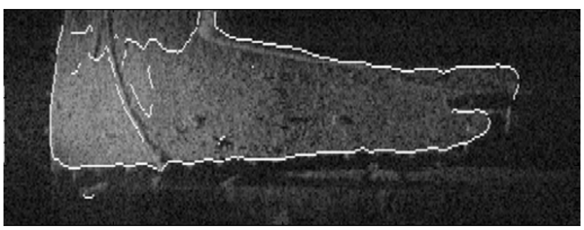

(d) Scale 8

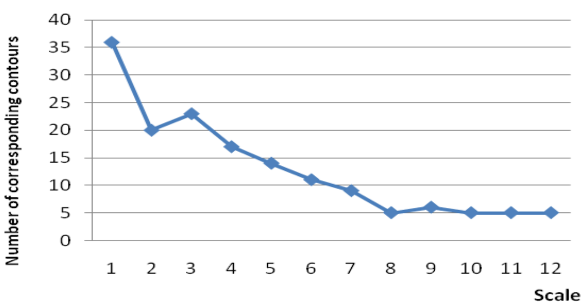

(e) Amount of corresponding contours versus scale

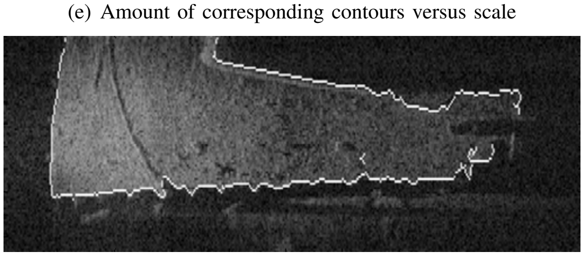

(f) Original corresponding contours still appearing at scale 8

Fig. 9. Multi-scale analysis for preserving scene relevant contours from *Bridge* sequence

(a) Scale 1 (original corresponding contours)

(b) Scale 2

(c) Scale 4

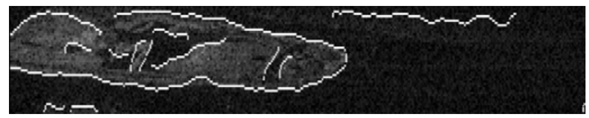

(d) Scale 6

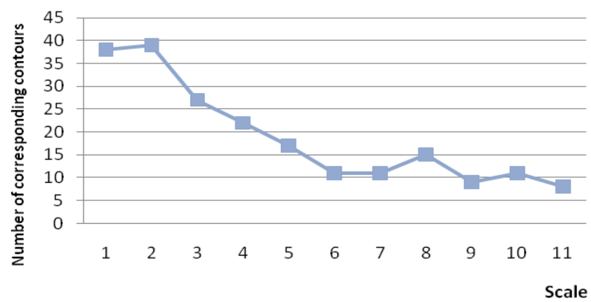

(e) Amount of corresponding contours versus scale

(f) Original corresponding contours still appearing at scale 6

Fig. 10. Multi-scale analysis for preserving scene relevant contours from *Ship* sequence

mogeneous matching chunks along the contour. Extra work is then required to split inhomogeneous contours in order to remove non-matching parts of contours.

V. Robust Feature Points Detection

A. Corners detectors algorithms

Many techniques have been developed for detecting [4] and chaining edges in order to further analyze their properties like taking points of high curvature to be labeled as corners [5]. A common approach for detecting high curvature points has been to use either one or two chords.

First techniques use a single chord spanning a fixed set of points in the chain to estimate the curve slope for each point of the curve and determine whether each point can be considered as isolated [6]. Corners are then defined as isolated discontinuities of the mean slope. Alternatively, pairs of chords can be computed to estimate the curve angle at their intersection [6]. Corners are then defined as local minima of these angles after local averaging. The pairs of chords defining the angle may have a central gap and only series of angle peaks (found by looking for zero crossings of angle values) spanning a few points, are defined as corners.

Other techniques do not use chords but apply smoothing filters to the curve. Corners are either the points with a high rate of slope change or points where the curvature decreases rapidly to the nearest minimum while keeping a small angle with the neighboring maxima [5].

B. *Proposed algorithm*

In this work, to find corners in selected edges, we use Douglas-Peucker algorithm also called Ramer-Douglas-Peucker algorithm or iterative end-point fit algorithm or split-and-merge algorithm.

The basic goal of this algorithm is to reduce the number of points in a curve, keeping only corner candidates (points with highest curvatures). Indeed, it recursively represents a curve as a series of more and more precise connected lines. Marking the first and last points of the curve as corners, it finds the furthest curve point away from the line defined by the two corners. If the distance between this point and the line is larger than a predefined threshold, this point is marked as corner and the splitting process is applied to the left and to the right part of the curve. If not, all the points between the two corners can be discarded as the smoothed curve (without these points) will not be further from the initial curve than the specified distance [7].

C. *Results and discussion*

Figures 11 and 12 show how the proposed algorithm performs on the previously extracted corresponding contours. As these contours are representative of scene elements edges, extracting corners from them detects salient points on these edges. These edges will be crucial for reconstructing the real scene shape and later for scene recognition and identification.

A first visual analysis of the results allows an easy identification of corresponding image corners. Indeed, the majority of detected corners from two successive frames (i and i+1) are located in almost the same positions, reducing the complexity of an automatic matching.

However, the goal of our work is to reconstruct the observed scene using multiple images acquired from different views and then from further frames. Thus, corners have been extracted from a third frame (i+15). The last images of Figures 11 and 12 show that globally the same set of corners is found, allowing a robust matching and then more accurate triangulations in order to 3D reconstruct the observed scene. These results of robust corners extraction and matching are very promising and allow testing the next steps of the proposed 3D reconstruction methodology with confidence.

(a) Frame i

(b) Frame i+1

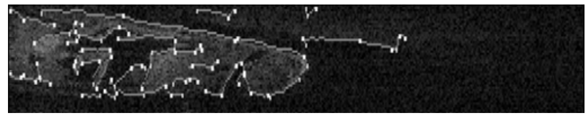

(c) Frame i+15

Fig. 11. Feature points extraction from *Ship* sequence

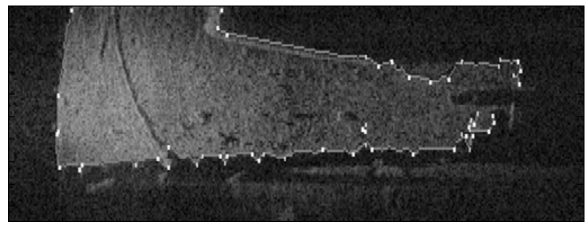

(a) Frame i

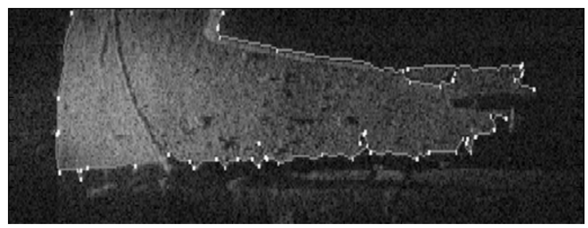

(b) Frame i+1

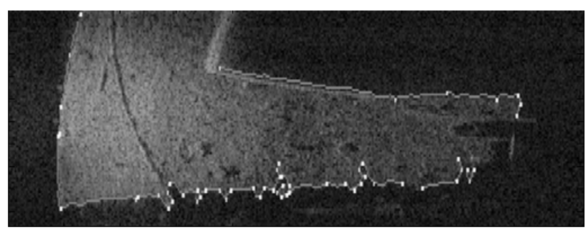

(c) Frame i+15

Fig. 12. Feature points extraction from *Bridge* sequence

VI. CONCLUSION

This paper presented a methodology to extract robust feature points that enable 3D reconstruction of underwater scenes using sequences of acoustic images. The approach relies on contours extraction as scene salient points logically appear on these contours. However, edge extraction often ends up at numerous false contours coming from noise. Thus, a multi-scale analysis combined to close images integration has been proposed to get relevant final contours robustly detecting scene geometric features. Using neighboring frames allows reducing the amount of contours resulting from noise as they will not appear identically on the two slightly shifted images. Indeed, only contours sharing common locations are preserved. Embedding this processing within a multi-scale approach, produces series of corresponding contours at several resolution scales. Only the corresponding contours from scale 1 still appearing at the deepest scale are kept as they represent strong scene geometric features. The final step consists in extracting corners from these contours as feature points.

This procedure produces interesting results as the sets of feature points extracted from different, non-neighboring frames seem to be consistent allowing an easy matching and then computing the geometric transformation between the corresponding attitudes and locations of the camera. Obviously, some scene features are missing from extracted corners to fully describe the scene topography but the procedure succeeds as enough robust points remain to compute the geometrical transformation between acquisition view points. Once this transformation been computed, it is still possible to come back and extract more feature points in order to complete the 3D reconstructed scene. The key feature of the proposed approach is to feed the algorithm responsible for determining this geometrical transformation, with robust and accurate pairs of points, corresponding to the same geographic location within the observed scene (salient points on sonar images). This methodology has been applied to real images showing very promising results for a full 3D scene reconstruction.

VII. Future work

As mentioned, dealing with inhomogeneous corresponding contours needs to be addressed to improve edge characterization and increase extracted feature points accuracy.

Finally, the extracted corners will feed the two last steps of the proposed global methodology which consist in computing the pose differences (translation & rotation) between two non-neighboring frames in order to compute the (x,y,z) scene coordinates of each salient point associated with a pair of corners.

A first trial has been made using simulated sonar images [8] on which the presented process has been run to obtain robust corners as shown in Figure 13. Finding the inter-acquisition geometry relies on minimizing the distance between the reconstructed points from image 1 and the image 2 reconstructed points according to a supposed translation & rotation. First rough results presented in Figure 14 show a preserved consistency of the overall geometry of the observed cube, even if a global bias appears. However, this first reconstructed scene offers promising perspectives.

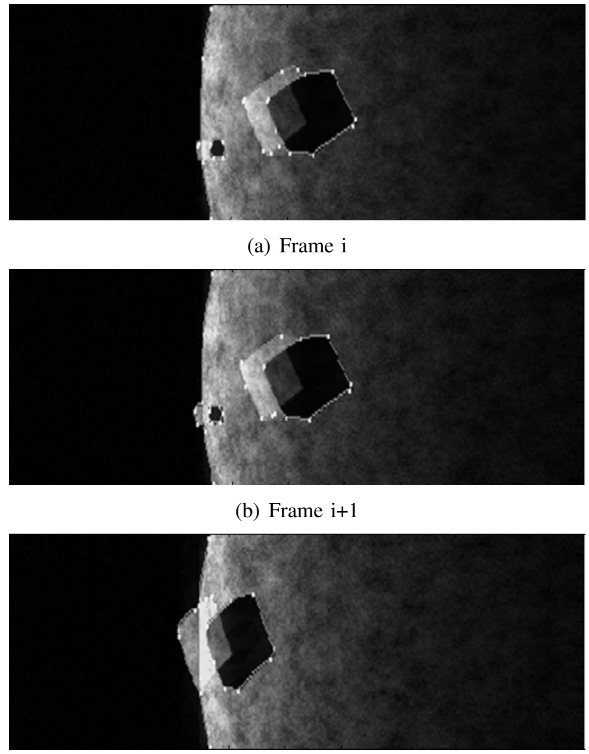

(a) Frame i

(b) Frame i+1

(c) Frame i+15

Fig. 13. Feature points extraction from a simulated acoustic camera sequence

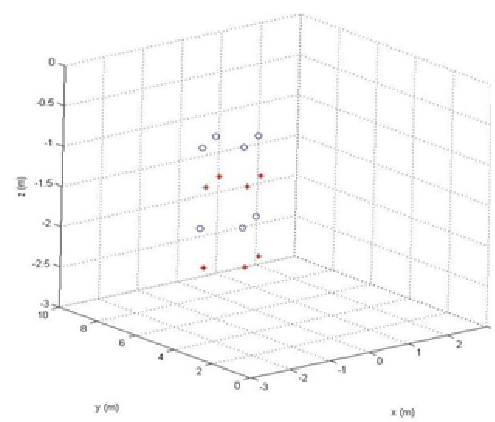

Fig. 14. Cube 3D reconstruction Cube - (o): Real points location - (*) : Reconstructed points location

References

[1] E. Belcher, W. Hanot, and J. Burch, “Dual-frequency identification sonar DIDSON,” *Underwater Technology, 2002. Proceedings of the 2002 International Symposium on*, pp. 187–192, 2002.

[2] K. Kim, N. Neretti, and N. Intrator, “Mosaicing of acoustic camera images,” *Radar, Sonar and Navigation, IEE Proceedings -*, vol. 152, no. 4, pp. 263–270, 5 Aug. 2005.

[3] J. Canny, “A computational approach to edge detection,” *Pattern Analysis and Machine Intelligence, IEEE Transactions on*, vol. PAMI-8, no. 6, pp. 679 –698, nov. 1986.

[4] X. Gao, F. Sattar, and R. Venkateswarlu, “Multiscale corner detection of gray level images based on log-gabor wavelet transform,” *Circuits and Systems for Video Technology, IEEE Transactions on*, vol. 17, no. 7, pp. 868 –875, july 2007.

[5] X. C. He and N. H. C. Yung, “Corner detector based on global and local curvature properties,” *Optical Engineering*, vol. 47, no. 5, p. 057008, 2008. [Online]. Available: http://link.aip.org/link/?JOE/47/057008/1

[6] E. Rosten, R. Porter, and T. Drummond, “Faster and better: A machine learning approach to corner detection,” *Pattern Analysis and Machine Intelligence, IEEE Transactions on*, vol. 32, no. 1, pp. 105 –119, jan. 2010.

[7] J. Hershberger and J. Snoeyink, “Speeding up the douglas-peucker line-simplification algorithm,” in *Proc. 5th Intl. Symp. on Spatial Data Handling*, 1992, pp. 134–143.

[8] D. Gueriot, C. Sintes, and R. Garello, “Sonar data simulation based on tube tracing,” in *OCEANS 2007 - Europe*, 18-21 June 2007, pp. 1–6.